

1 **ChAdOx1 nCoV-19 (AZD1222) protects Syrian hamsters against SARS-CoV-2 B.1.351 and**
2 **B.1.1.7**

3 Robert J. Fischer^{1†}, Neeltje van Doremalen^{1†}, Danielle R. Adney^{1†}, Claude Kwe Yinda¹, Julia R.
4 Port¹, Myndi G. Holbrook¹, Jonathan E. Schulz¹, Brandi N. Williamson¹, Tina Thomas¹, Kent
5 Barbian², Sarah L. Anzick², Stacy Ricklefs², Brian J. Smith³, Dan Long³, Craig Martens², Greg
6 Saturday³, Emmie de Wit¹, Sarah C. Gilbert⁴, Teresa Lambe⁴, Vincent J. Munster^{1*}

7

8 1. Laboratory of Virology, National Institute of Allergy and Infectious Diseases,
9 National Institutes of Health, Hamilton, MT, USA.

10 2. Research Technologies Branch, Rocky Mountain Laboratories, National Institutes of
11 Health, Hamilton, Montana, USA.

12 3. Rocky Mountain Veterinary Branch, National Institute of Allergy and Infectious
13 Diseases, National Institutes of Health, Hamilton, MT, USA.

14 4. The Jenner Institute, Nuffield Department of Medicine, University of Oxford, Oxford,
15 UK.

16

17 †=These authors contributed equally

18 *=Corresponding author

19

20 **Abstract**

21 We investigated ChAdOx1 nCoV-19 (AZD1222) vaccine efficacy against SARS-CoV-2 variants
22 of concern (VOCs) B.1.1.7 and B.1.351 in Syrian hamsters. We previously showed protection
23 against SARS-CoV-2 disease and pneumonia in hamsters vaccinated with a single dose of
24 ChAdOx1 nCoV-19. Here, we observed a 9.5-fold reduction of virus neutralizing antibody titer
25 in vaccinated hamster sera against B.1.351 compared to B.1.1.7. Vaccinated hamsters challenged
26 with B.1.1.7 or B.1.351 did not lose weight compared to control animals. In contrast to control
27 animals, the lungs of vaccinated animals did not show any gross lesions. Minimal to no viral
28 subgenomic RNA (sgRNA) and no infectious virus was detected in lungs of vaccinated animals.
29 Histopathological evaluation showed extensive pulmonary pathology caused by B.1.1.7 or
30 B.1.351 replication in the control animals, but none in the vaccinated animals. These data
31 demonstrate the effectiveness of the ChAdOx1 nCoV-19 vaccine against clinical disease caused
32 by B.1.1.7 or B.1.351 VOCs.

33

34 **Main**

35 The COVID-19 pandemic produced an unprecedented development of SARS-CoV-2 vaccines,
36 and just over a year after the beginning of the outbreak a total of 12 vaccines have been
37 authorized or approved globally. As the pandemic progressed, several variants of concern
38 (VOCs) have been detected. These include the B.1.1.7 and B.1.351 VOCs. The B.1.1.7 VOC was
39 first detected in the United Kingdom and has seven amino acid (AA) substitutions and two
40 deletions in the spike protein^{1,2} compared to the original Wuhan isolate, Wuhan-Hu-1. The
41 B.1.351 VOC was first detected in South Africa and has eight AA substitutions and one deletion
42 in the spike protein³ (Table 1). All currently licensed vaccines are based on the spike protein of

43 Wuhan-Hu-1, thus, concerns have been raised that the presence of these changes may affect
44 vaccine efficacy. The goal of this study was to evaluate ChAdOx1 nCoV-19 (AZD1222) vaccine
45 efficacy in Syrian hamsters, when challenged using naturally occurring isolates of the VOCs
46 B.1.1.7 and B.1.351.

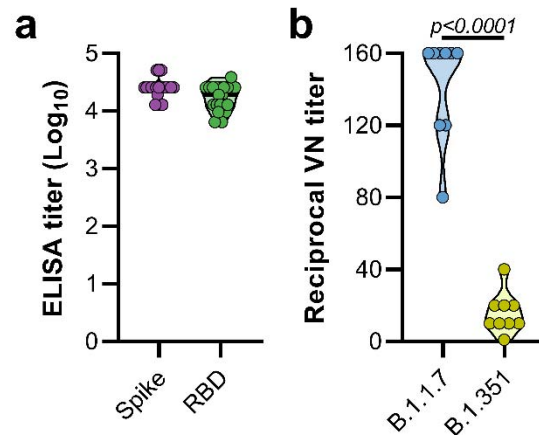
47

Substitution (Wuhan AA numbering)	VOC B.1.1.7¹	VOC B.1.351³
L18F	-	+
HV69-70del	+	-
D80A	-	+
Y144del	+	-
D215G	-	+
LAL242-244del	-	+
K417N	-	+
E484K	-	+
N501Y	+	+
A570D	+	-
D614G	+	+
P681D	+	-
A701V	-	+
T716I	+	-
S982A	+	-
D1118H	+	-

48 Table 1. AA substitutions detected in the spike protein of VOCs B.1.1.7 (EPI_ISL_601443) and
49 B.1.351 (EPI_ISL_678615) compared to Wuhan-Hu-1 (NC_045512).

50

51 Syrian hamsters (N=10 per group) were vaccinated intramuscularly with either ChAdOx1 nCoV-
52 19 or ChAdOx1 green fluorescent protein (GFP, 2.5×10^8 IU/hamster) 30 days prior to intranasal
53 challenge with SARS-CoV-2. Vaccination with ChAdOx1 nCoV-19 resulted in high titers of
54 binding antibodies against the SARS-CoV-2 full-length spike protein and receptor binding
55 domain (Figure 1a) at 25 days post vaccination. We then investigated neutralizing antibody titers
56 in serum against infectious virus. Neutralization of B.1.351 was significantly reduced compared
57 to neutralization of B.1.1.7 (Figure 1b, mean titer of 15 vs 142, $p < 0.0001$, Mann-Whitney test).



58

59 **Figure 1. Vaccination of Syrian hamsters with ChAdOx1 nCoV-19 elicits binding and**
60 **neutralizing antibodies against B.1.1.7 and B.1.351.** a. Violin plot of binding antibodies
61 against spike protein or RBD of SARS-CoV-2 (clade A) in serum obtained 25 days post
62 vaccination with ChAdOx1 nCoV-19. b. Violin plot of virus neutralizing antibody titers against
63 B.1.1.7 or B.1.351 in serum obtained 25 days post vaccination with ChAdOx1 nCoV-19.
64 Statistical significance determined via Kruskal-Wallis test.

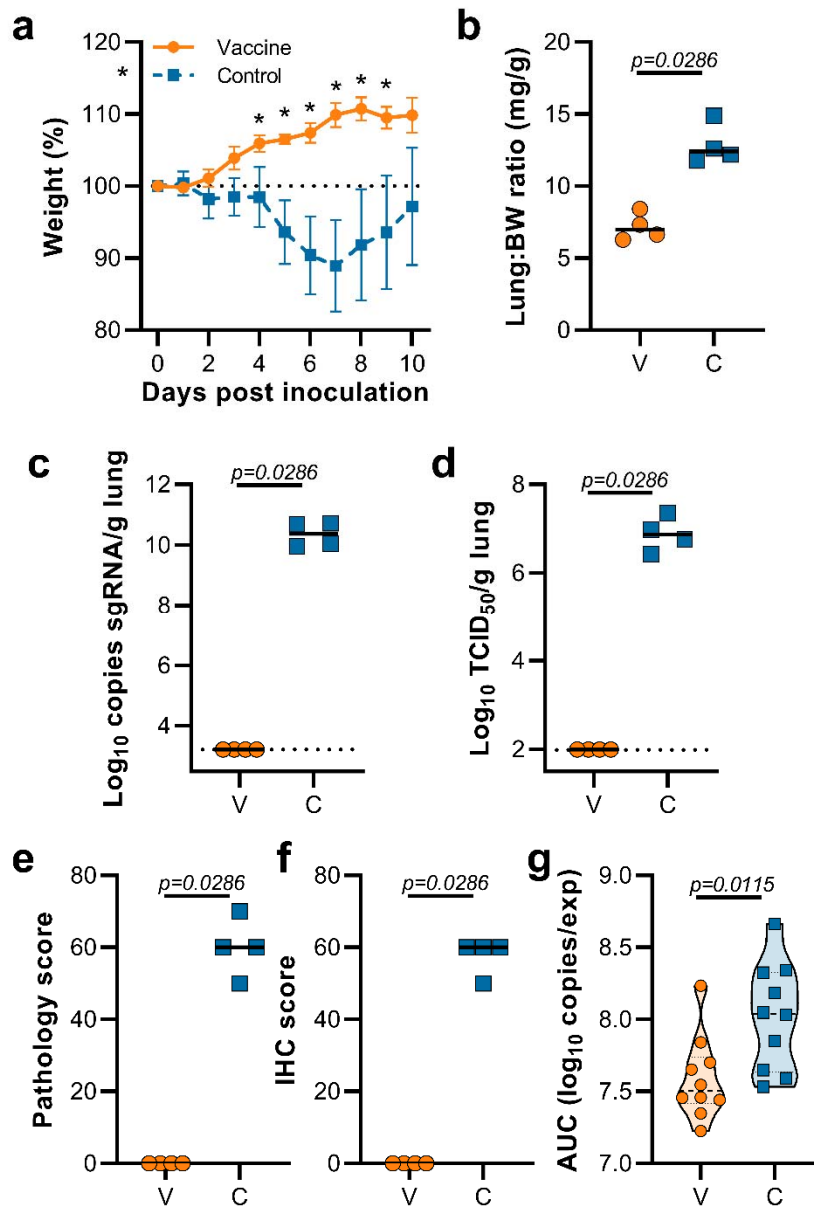
65

66 ***ChAdOx1 nCoV-19 vaccinated hamsters are protected against lower respiratory tract infection***
67 ***with B.1.1.7***

68 Hamsters were inoculated with B.1.1.7 via the intranasal route. Weight loss was observed in
69 control hamsters whereas vaccinated hamsters continued to gain weight throughout the
70 experiment (Figure 2a). A significant difference in weight between vaccinated and control
71 hamsters was observed starting at 4 days post infection (DPI) for B.1.1.7 (Figure 2a, Student's t-
72 test corrected for multiple comparisons using the Holm-Šidák method) and continued throughout
73 the remainder of the experiment. Four out of ten hamsters per group were euthanized at 5 DPI
74 and lung tissue was harvested. Lung:body weight ratios on 5 DPI were significantly lower in
75 vaccinated animals compared to control animals (Figure 2b, $p=0.0286$, Mann-Whitney test),
76 indicating no or reduced pulmonary edema in ChAdOx1 nCoV19-vaccinated animals. Lung
77 tissue of all control animals contained high levels of sgRNA (Figure 2c, 10^{10} copies/gram tissue),

78 and was comparable to sgRNA levels previously detected in lung tissue of control animals
79 challenged with SARS-CoV-2 D614G (hCoV-19/USA/MT-RML-7/2020)⁴. Conversely, no
80 sgRNA was detected in lung tissue obtained from vaccinated hamsters challenged with B.1.1.7
81 (Figure 2c, $p=0.0286$, Mann-Whitney test). High levels of infectious virus were detected in lung
82 tissue of all control animals, whereas no vaccinated animals had detectable infectious virus in
83 lung tissue (Figure 2d, $p=0.0286$, Mann-Whitney test).

84 Lung tissue was then evaluated for histology. The percentage of lung tissue that showed
85 pathology and the percentage of lung tissue that was positive for SARS-CoV-2 antigen was
86 determined by a veterinary pathologist blinded to the study group allocations. Whereas no
87 pathology nor SARS-CoV-2 antigen was found in lung tissue of vaccinated animals, this was
88 abundantly present in lung tissue of control animals (Figure 2e,f). Finally, oropharyngeal swabs
89 were collected on 1 to 5 DPI, evaluated for sgRNA, and an area under the curve was calculated
90 per animal to determine the total amount of virus shed. We observed a significant decrease in the
91 total amount of virus found in oropharyngeal swabs from vaccinated animals compared to
92 control animals (Figure 2g, Mann-Whitney test).



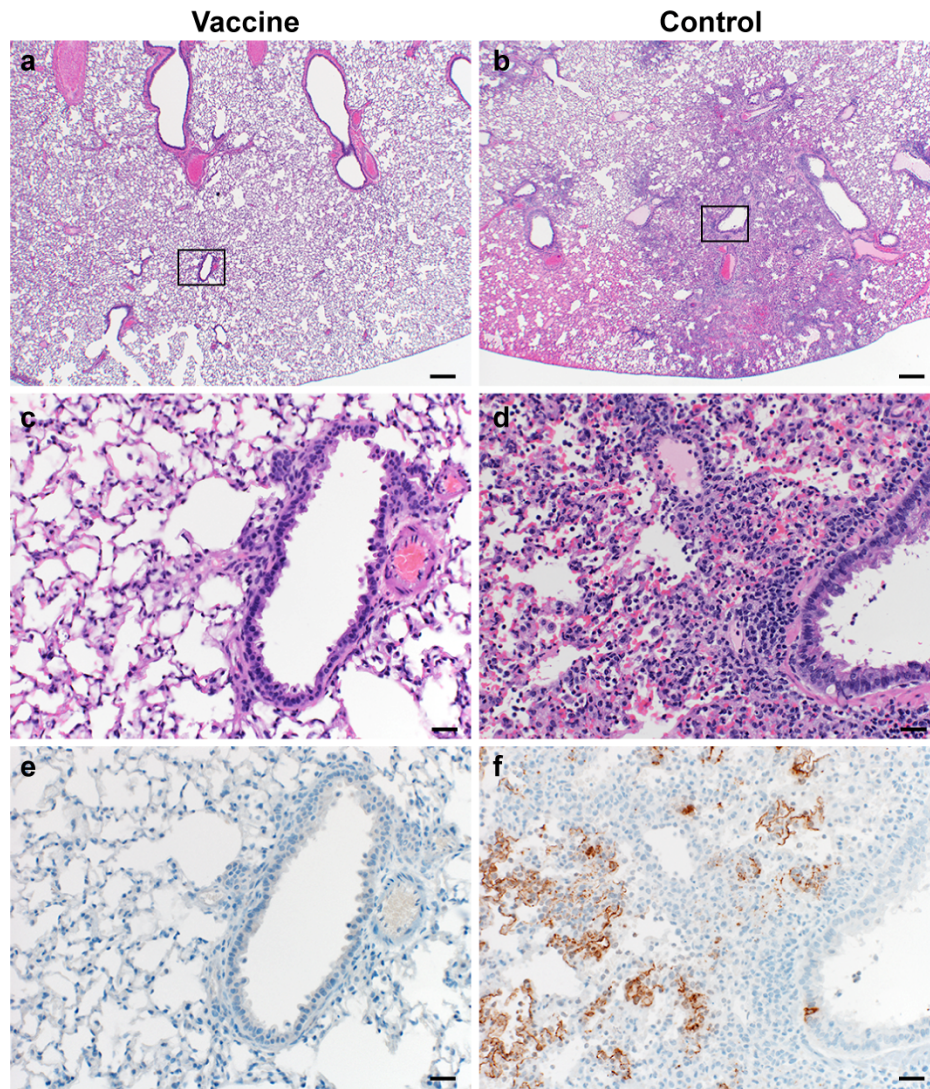
93

94 **Figure 2. Vaccination of Syrian hamsters with ChAdOx1 nCoV-19 prevents lower**
 95 **respiratory tract infection with SARS-CoV-2 VOC B.1.1.7.** a. Relative weight upon intranasal
 96 challenge with 10^4 TCID₅₀ of B.1.1.7. Shown is geometric mean with 95% confidence interval
 97 (CI). * = p-value < 0.05, corrected for multiple comparisons using the Holm-Šidák correction. b.
 98 Lung:body weight (BW) ratio (mg:g) of hamsters euthanized at 5 DPI. Line = median. c. sgRNA
 99 viral load in lung tissue obtained at 5 DPI. Line = median. Dotted line = limit of detection. d.
 100 Infectious SARS-CoV-2 titer in lung tissue obtained at 5 DPI. Line = median. Dotted line = limit
 101 of detection. e. Percentage affected lung tissue per animal as determined via histology. Line =
 102 median. f. Percentage of lung tissue positive for SARS-CoV-2 antigen per animal. Line =

103 median. g. Truncated violin plot of area under the curve (AUC) analysis of shedding as measured
104 by sgRNA analysis in swabs collected on 1 – 5 dpi. Dashed line = median. Dotted line =
105 quartiles. Statistical significance determined via mixed-effect analyses (a), or Mann-Whitney test
106 (b-g). V = ChAdOx1 nCoV-19 vaccinated; C = ChAdOx1 GFP vaccinated; Orange circle =
107 Hamsters vaccinated with ChAdOx1 nCoV-19, Blue square = Hamsters vaccinated with
108 ChAdOx1 GFP.

109

110 Lung tissue was then evaluated for histology. Microscopically, pulmonary lesions of control
111 animals consisted of a moderate to marked broncho-interstitial pneumonia extending into the
112 adjacent alveoli previously observed in hamsters inoculated with SARS-CoV-2 WA1 or a
113 D614G isolate^{4,5}. Bronchi and bronchioles had multifocal necrotic epithelial cells and moderate
114 numbers of infiltrating neutrophils and macrophages. Alveolar septa were expanded by edema
115 fluid and leucocytes. In contrast, vaccinated animals did not show any evidence of SARS-CoV-2
116 pathology (Figure 3a-d). Immunohistochemistry using a monoclonal antibody against SARS-
117 CoV-2 demonstrated viral antigen in bronchial and bronchiolar epithelium, type I and II
118 pneumocytes as well as pulmonary macrophages within the control animals, but not in
119 vaccinated animals (Figure 3e-f).



120

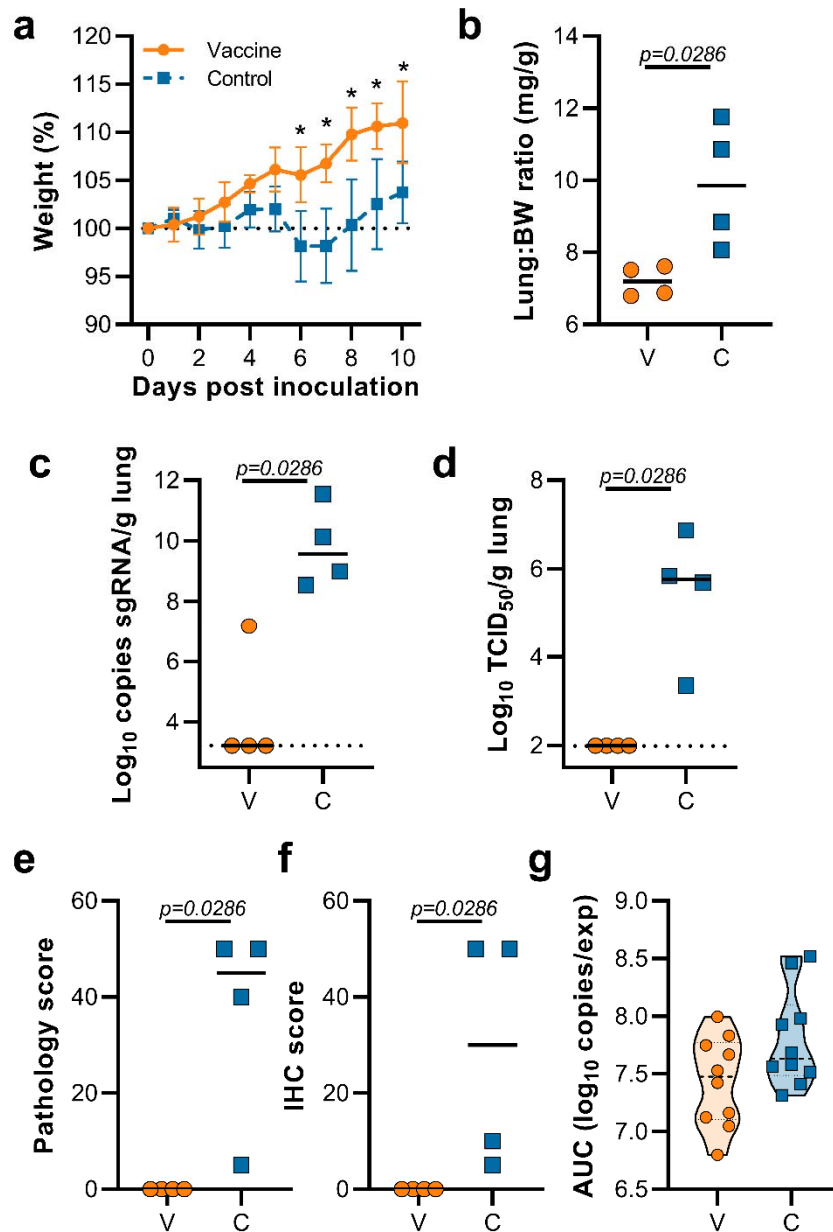
121 **Figure 3. Pulmonary effects of direct intranasal challenge with SARS-CoV-2 variant**
122 **B.1.1.7 in Syrian hamsters at 5 DPI.** a-b. H&E staining, 20x; a. No pathology. b. Focally
123 extensive areas of bronchointerstitial pneumonia. c-d. H&E staining, 200x; c. No pathology. d.
124 Bronchointerstitial pneumonia with alveolar histiocytosis, fibrin and edema. e-f. IHC staining
125 against N protein SARS-CoV-2 (brown). e. No staining. f. Staining of bronchiolar epithelial
126 cells, type I&II pneumocytes and rare macrophages.
127

128 *ChAdOx1 nCoV-19 vaccinated hamsters are protected against lower respiratory tract infection*
129 *with B.1.351*

130 This experiment was repeated using B.1.351 (isolate hCoV-19/South Africa/KRISP-

131 K005325/2020) instead of B.1.1.7 as an inoculation virus. Two AA substitutions were found in

132 the spike protein of the B.1.351 virus stock; Q677H (present at 88%) and R682W (present at
133 89%). A lack of weight gain was observed in control hamsters, but not vaccinated hamsters,
134 which was significant starting at 6 DPI (Figure 4a, Student's t-test corrected for multiple
135 comparisons using the Holm-Šidák method). Four out of ten hamsters per group were euthanized
136 at 5 DPI and lung tissue was harvested. Lung:body weight ratios were significantly lower in
137 vaccinated animals compared to control animals (Figure 4b, $p=0.0286$, Mann-Whitney test).
138 Lung tissue of all control animals contained high levels of sgRNA, but only one vaccinated
139 animal had relative low levels of sgRNA in lungs (Figure 4c, $p=0.0286$, Mann-Whitney test).
140 Likewise, high levels of infectious virus were detected in lungs of control animals, but not in
141 lungs of vaccinated animals (Figure 4d, $p=0.0286$, Mann-Whitney test). As in the previous
142 experiment, no pathology nor SARS-CoV-2 antigen was found in lung tissue of vaccinated
143 animals compared to control animals (Figure 4e,f, $p=0.0286$, Mann-Whitney test). No decrease
144 in the total amount of virus found in oropharyngeal swabs from vaccinated animals compared to
145 control animals was found (Figure 4g, Mann-Whitney test).
146



147

148 **Figure 4. Vaccination of Syrian hamsters with ChAdOx1 nCoV-19 prevents lower**
149 **respiratory tract infection with SARS-CoV-2 VOC B.1.351.** a. Relative weight upon
150 intranasal challenge with 10^4 TCID₅₀ of B.1.351. Shown is geometric mean with 95% confidence
151 interval (CI). * = p -value<0.005, corrected for multiple comparisons using the Holm-Šidák
152 correction. b. Lung:body weight (BW) ratio (mg:g) of hamsters euthanized at 5 DPI. Line =
153 median. c. sgRNA viral load in lung tissue obtained at 5 DPI. Line = median. Dotted line = limit
154 of detection. d. Infectious SARS-CoV-2 titer in lung tissue obtained at 5 DPI. Line = median.
155 Dotted line = limit of detection. e. Percentage affected lung tissue per animal as determined via

156 histology. Line = median. f. Percentage of lung tissue positive for SARS-CoV-2 antigen per
157 animal. Line = median. g. Truncated violin plot of area under the curve (AUC) analysis of
158 shedding as measured by sgRNA analysis in swabs collected on 1 – 5 dpi. Dashed line = median.
159 Dotted line = quartiles. Statistical significance determined via mixed-effect analyses (a), or
160 Mann-Whitney test (b-g). V = ChAdOx1 nCoV-19 vaccinated; C = ChAdOx1 GFP vaccinated;
161 Orange circle = Hamsters vaccinated with ChAdOx1 nCoV-19, Blue square = Hamsters
162 vaccinated with ChAdOx1 GFP.

163

164 We investigated the presence of the AA substitutions Q677H and R682W observed in 88-89% of
165 the spike protein of our B.1.351 stock in swabs and lung tissue obtained from control animals
166 challenged. Whereas we did find these substitutions in swabs obtained at 1 DPI, they were not
167 present in swabs obtained at 5 DPI. Likewise, the substitutions were only found in lung tissue of
168 one out of four control hamsters (Table 2).

169

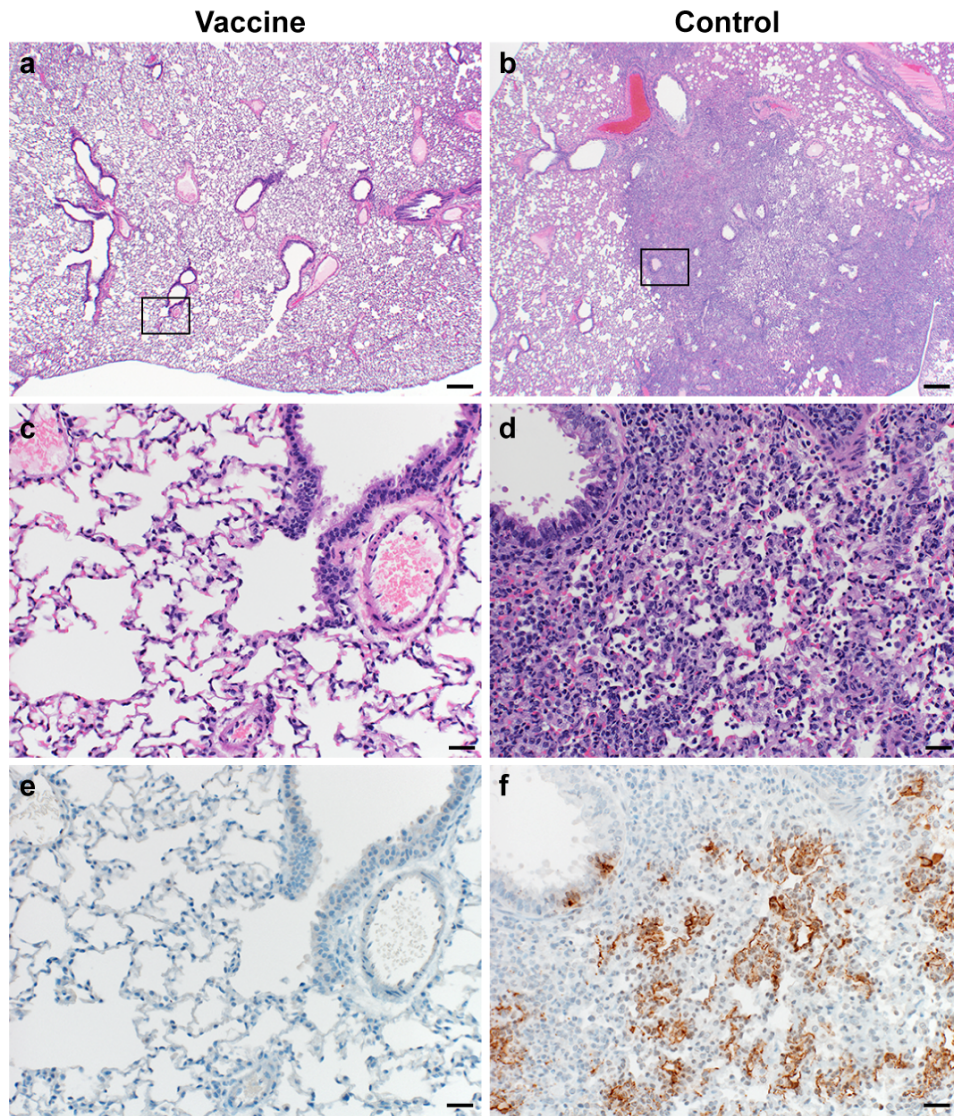
AA substitutions	Presence in swabs (1 DPI, N=5)	Presence in swabs (5 DPI, N=3)	Presence in lungs (N=4)
Q677H	44.1-65.7%	0%	0 (N=3), 81% (N=1)
R682W	44.9-65.8%	0%	0 (N=3), 81% (N=1)

170 Table 2. Presence of substitutions Q677H and R682W in swabs and lung tissue of hamsters
171 directly inoculated with B.1.351.

172

173 Lung tissue was then evaluated for histology. Microscopically, pulmonary lesions of control
174 animals were comparable to results obtained from previous SARS-CoV-2 infections of hamsters.
175 In contrast, vaccinated animals did not show any evidence of SARS-CoV-2 pathology (Figure
176 5a-d). Likewise, immunohistochemistry demonstrated viral antigen present in bronchial and
177 bronchiolar epithelium, type I and II pneumocytes as well as pulmonary macrophages within the
178 control animals, but not in vaccinated animals (Figure 5e-f).

179



180

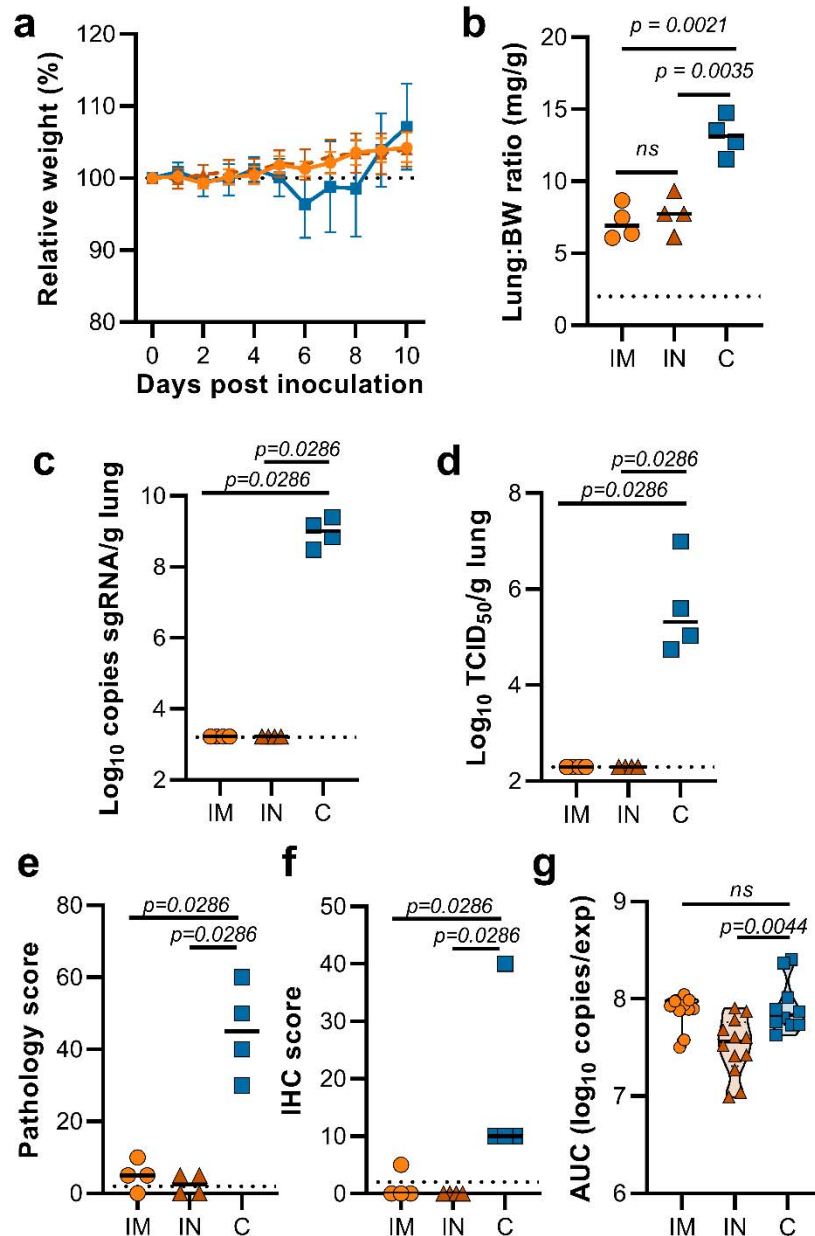
181 **Figure 5. Pulmonary effects of direct intranasal challenge with SARS-CoV-2 variant**
182 **B.1.351 in Syrian hamsters at 5 DPI.** a-b. H&E staining, 20x; a. No pathology. b. Focally
183 extensive areas of bronchointerstitial pneumonia. c-d. H&E staining, 200x; c. No pathology. d.
184 Bronchointerstitial pneumonia with alveolar histiocytosis, fibrin and edema. e-f. IHC staining
185 against SARS-CoV-2 (brown). e. No staining. f. Staining of bronchiolar epithelial cells, type
186 I&II pneumocytes and rare macrophages.

187

188

189 *Hamsters vaccinated with ChAdOx1 nCoV-19 via the intranasal route are protected against*
190 *lower respiratory tract infection with B.1.351*

191 Intranasal vaccination of hamsters with ChAdOx1 nCoV-19 resulted in a reduction of shedding
192 of SARS-CoV D614G⁴. We hypothesized that a similar reduction in shedding would be found
193 upon inoculation with B.1.351. Animals were vaccinated with 2.5×10^8 IU ChAdOx1 nCoV-
194 19/animal, either via the intranasal route or via the intramuscular route. A new stock of B.1.351
195 was obtained, and next gen sequencing revealed no SNPs in the spike protein (isolate hCoV-
196 19/USA/MD-HP01542/2021) from here on referred to as B.1.351-2. Sixty days post vaccination,
197 animals were challenged with 10^4 TCID₅₀ of B.1.351-2. As a control group, naïve animals were
198 inoculated. Weight loss was minimal in control animals, and absent in vaccinated animals
199 (Figure 6a). At 5 DPI, four animals per group were euthanized. Compared to control animals,
200 lung:BW ratio of vaccinated animals was significantly reduced, and there was no difference
201 between the two vaccine groups (Figure 6b). No viral sgRNA or infectious virus was detected in
202 lung tissue of vaccinated animals, whereas it was abundantly present in lung tissue of control
203 animals (Figure 6c-d). As shown in the previous experiment, no difference in the amount of virus
204 shed was found when animals were vaccinated via the IM route. In contrast, a significant
205 reduction was found in animals vaccinated via the IN route (Figure 6g).
206



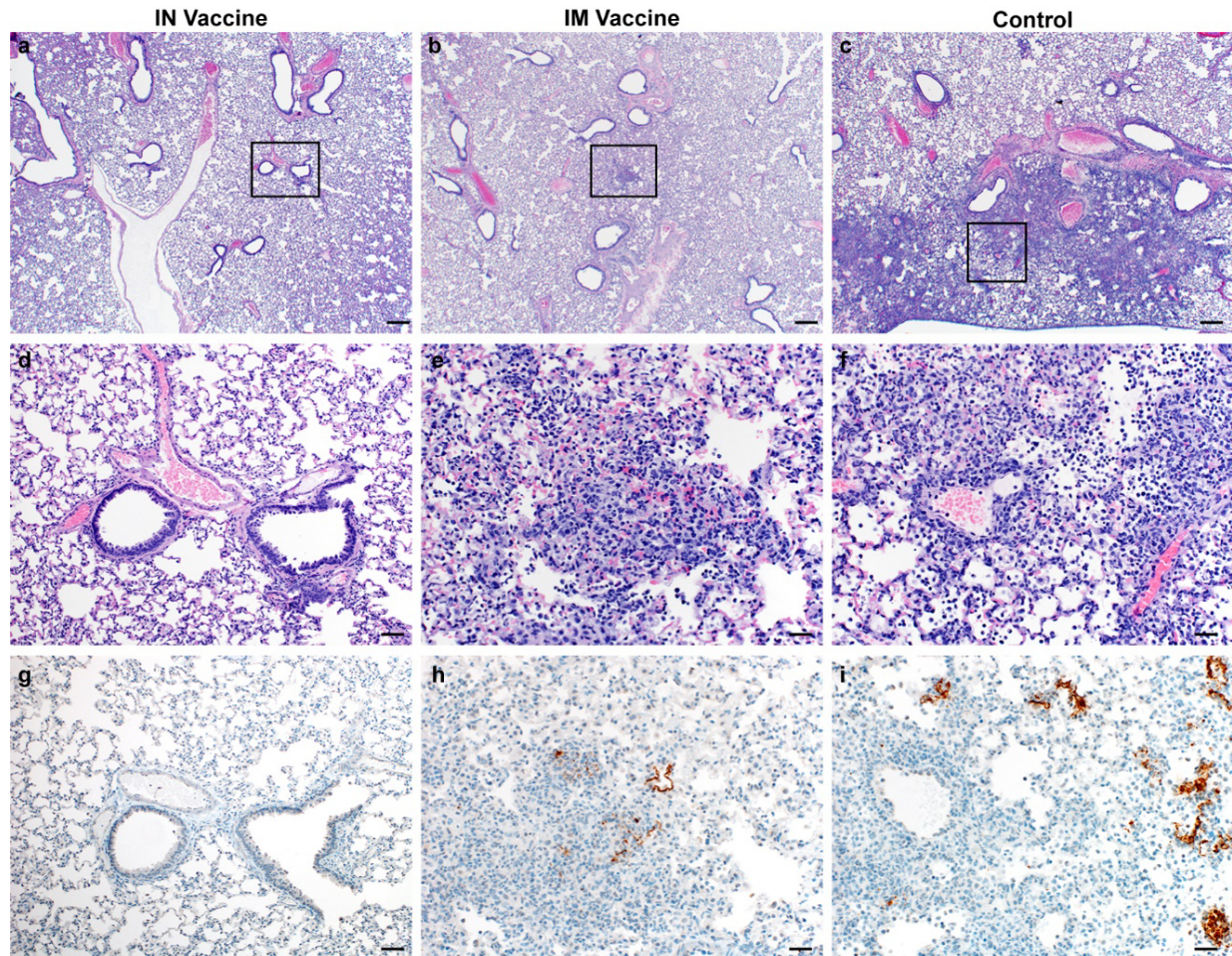
207

208 **Figure 6. Vaccination of Syrian hamsters with ChAdOx1 nCoV-19 via the IM or IN route**
 209 **prevents lower respiratory tract infection with SARS-CoV-2 VOC B.1.351-2.** Hamsters were
 210 vaccinated by the IM or the IN routes 60 days prior to challenge with B.1.351-2. a. Relative
 211 weight upon intranasal challenge with 10^4 TCID₅₀ of B.1.351. Shown is geometric mean with
 212 95% confidence interval (CI). * = p -value < 0.005, corrected for multiple comparisons using the
 213 Holm-Šidák correction. b. Lung:body weight (BW) ratio (mg:g) of hamsters euthanized at 5 DPI.
 214 Line = median. c. sgRNA viral load in lung tissue obtained at 5 DPI. Line = median. Dotted line
 215 = limit of detection. d. Infectious SARS-CoV-2 titer in lung tissue obtained at 5 DPI. Line =

216 median. Dotted line = limit of detection. e. Percentage affected lung tissue per animal as
217 determined via histology. Line = median. f. Percentage of lung tissue positive for SARS-CoV-2
218 antigen per animal. Line = median. g. Truncated violin plot of area under the curve (AUC)
219 analysis of shedding as measured by sgRNA analysis in swabs collected on 1 – 5 DPI. Dashed
220 line = median. Dotted line = quartiles. Statistical significance determined via mixed-effect
221 analyses (a), or Mann-Whitney test (b-g). IM = ChAdOx1 nCoV-19 vaccinated via intramuscular
222 route; IN = ChAdOx1 nCoV-19 vaccinated via intranasal route; C = naïve animals; Orange circle
223 = Hamsters vaccinated with ChAdOx1 nCoV-19 via intramuscular route, Orange triangle =
224 Hamsters vaccinated with ChAdOx1 nCoV-19 via intranasal route, Blue square = Naïve
225 hamsters.

226

227 Histopathology of the lungs collected 5 DPI show pulmonary lesions of control animals with a
228 moderate to marked broncho-interstitial pneumonia extending into the adjacent alveoli. Bronchi
229 and bronchioles had multifocal necrotic epithelial cells and scattered to numerous infiltrating
230 neutrophils and macrophages. Alveolar septa were expanded by edema fluid and
231 leucocytes (Figure 7c&f). IN vaccinated animals did not show any evidence of SARS-CoV-2
232 pathology (Figure 7a&d). IM vaccinated animals had rare foci of interstitial pneumonia (Figure
233 7b&e). Immunohistochemistry using a monoclonal antibody against SARS-CoV-2 demonstrated
234 moderate to numerous viral antigen in bronchial and bronchiolar epithelium, scattered to
235 numerous type I and II pneumocytes as well as rare pulmonary macrophages within the control
236 animals. The IM vaccinated animals had none to rare instances of type I and II pneumocytes and
237 pulmonary macrophages while the IN vaccinated animals showed no evidence of viral antigen in
238 the lungs (Figure 7g-i).



239

240 **Figure 7. Pulmonary effects of direct IN challenge with SARS-CoV-2 variant B.1.351 in**
241 **Syrian hamsters which received an IN or IM vaccine at 5 DPI. a-c: H&E 20x; a. No**
242 **pathology. b-c. general prevalence of interstitial pneumonia. d-f H&E 200x; d. No pathology e.**
243 **rare focus of interstitial pneumonia. f. moderate interstitial pneumonia. g-i. IHC staining against**
244 **N protein SARS-CoV-2, 200x. g. No viral antigen. h. Rare foci of viral antigen in type I**
245 **pneumocytes. i. Viral antigen within the larger area of interstitial pneumonia in type I**
246 **pneumocytes (20x bar = 200 μ m; 200x bar = 20 μ m).**

247 This study demonstrates efficacy of the ChAdOx1 nCoV-19 vaccine against circulating variants
248 of concern in the SARS-CoV-2 Syrian hamster model. The Syrian hamster SARS-CoV-2
249 infection model is characterized by natural susceptibility to SARS-CoV-2 and development of a
250 robust upper and lower respiratory tract infection⁶. The hamster model has been successfully
251 used for the preclinical development of several vaccines including the Ad26 and mRNA-1273
252 vaccines by Janssen⁷ and Moderna⁸, respectively. Several groups have reported the effect of

253 spike protein substitutions observed in B.1.1.7 and B.1.351 VOCs on the virus neutralizing
254 capacity of serum obtained from vaccinated or convalescent individuals. In general, these studies
255 conclude that the substitutions found in the B.1.1.7 spike protein have limited to no effect on
256 virus neutralization titres⁹⁻¹⁵. Data from a UK phase III trial taken from a time when B.1.1.7
257 predominated, showed minimal impact on ChAdOx1 nCoV-19 vaccine efficacy¹⁵. Likewise, in
258 an observational study of vaccine effectiveness in adults aged over 70 years in the UK, a single
259 dose of either ChAdOx1 nCoV-19 or the Pfizer/BioNTech vaccine BNT162b2 reduced
260 hospitalization in elderly adults with co-morbidities by 80%¹⁶. In contrast, the substitutions
261 found in the B.1.351 spike protein (Table 1) result in a significant reduction of virus neutralizing
262 capacity with pseudotype or infectious virus neutralization assays^{9-15,17,18}. The ChAdOx1 nCoV-
263 19 vaccine showed a 9 times reduction in neutralizing antibody titer against B.1.351 than against
264 an earlier variant circulating in South Africa^{10,19}. In a phase II study of ChAdOx1 nCoV-19 in
265 South Africa, in 2000 adults with a median age of 31 years, vaccine efficacy against mild to
266 moderate disease was reduced when the virus recovered after infection was B.1.351 (19 cases in
267 the vaccinated group and 20 in the placebo group)¹⁹. Vaccine efficacy against severe disease
268 could not be determined as no severe cases occurred in this young cohort. The South African arm
269 of the ENSEMBLE study which tested vaccine efficacy after a single dose of Janssen's COVID-
270 19 vaccine candidate enrolled 6,576 participants in South Africa, out of a total of 43,783 in
271 multiple countries, with 34% of participants across the study aged over 60 years. Vaccine
272 efficacy against moderate to severe disease was 64% (CI 41.2%, 78.7%) in South Africa
273 compared to 72% (CI 58.2%, 81.7%) in the USA at 28 days post vaccination²⁰. Efficacy of the
274 vaccine against severe to critical disease was 81.7% in South Africa, which was similar to the
275 reported 85.9% and 87.6% in the USA and Brazil, respectively²⁰. Vaccine efficacy against mild

276 disease was not reported. These clinical trial results are consistent with the findings of the
277 preclinical study reported here; ChAdOx1 nCov-19 may be less effective at reducing upper
278 respiratory tract infection caused by B.1.351 than by B.1.1.7, consistent with reduced efficacy
279 against mild disease. However, complete protection against lower respiratory tract disease was
280 observed in this challenge study, consistent with protection against severe disease. Based on our
281 data, we hypothesize that the currently available vaccines will likely still protect against severe
282 disease and hospitalization caused by VOC B.1.351.

283 Limited data on the immunological determinants of protection are available, however recent data
284 from rhesus macaques indicate that relatively low neutralizing antibody titers are sufficient for
285 protection against SARS-CoV-2, and that cellular immune responses may contribute to
286 protection if antibody responses are suboptimal²¹. Induction of binding and neutralizing
287 antibodies as well as SARS-CoV-2 cellular spike protein-specific T cell responses after
288 vaccination have been reported^{22,23} and most SARS-CoV-2 specific T cell epitopes in both
289 convalescent and vaccinated individuals are not affected by the AA substitutions found in the
290 spike protein of the B.1.1.7 and B.1.351 variants²⁴. Protection against severe COVID-19 disease
291 might be mediated by T cells and therefore may not be different between the current variants.
292 However, as T cell-mediated protection in the lower respiratory tract can only act after the initial
293 infection has occurred, mild, polymerase chain reaction (PCR)-positive disease may still occur in
294 the upper respiratory tract.

295 It should be noted that when the B.1.351 virus stock used to challenge hamsters contained two
296 additional non-fixed AA substitutions; Q677H and R682W at 88% and 89%, respectively. The
297 relative presence of these two AA substitutions was markedly reduced at 1 DPI and absent on 5
298 DPI. In addition, they were only present in lung tissue of one control hamster at 5 DPI,

329 suggesting that they are rapidly selected against in the SARS-CoV-2 hamster model over the
330 course of infection. Nonetheless, since the substitutions thought to be important in immune
331 evasion, such as E484K¹⁸, are still present in the virus stock, efficient replication and lung
332 pathology was observed in infected hamsters, we believe that conclusions can still be reached
333 from the data presented in Figure 3. Additionally, we used a B.1.351 stock without AA
334 mutations in the final experiments. Again, we did not find any disease in vaccinated hamsters
335 inoculated with B.1.351, whether they received an IN or an IM vaccination.

336 Interestingly, in this same study a reduction in viral detection in oropharyngeal swabs could be
337 detected in hamsters that received an IN vaccination, in contrast to hamsters that received an IM
338 vaccination. These results are in line with previous studies that were done at a shorter time frame
339 (25 and 28 days between vaccination and challenge)^{4,25}. Our study shows that these differences
340 last for at least 60 days post vaccination in hamsters, even with a VOC that has reduced the
341 neutralizing ability of antibodies in sera.

342 Based on the current studies and healthcare priorities in real-world settings, we believe it is
343 essential to focus on prevention of moderate to severe disease requiring hospitalization. We show
344 that ChAdOx1 nCoV-19 vaccination resulted in complete protection against disease in hamsters.
345 As implied by the data presented by Janssen²⁰, viral vectored vaccines may provide substantial
346 protection against lower respiratory tract infection caused by the B.1.351 variant and subsequent
347 hospitalization and death. With the ongoing evolution of SARS-CoV-2, the readily available and
348 cost-effective hamster model allows rapid evaluation of the protective efficacy of novel VOCs.
349 In addition, it will allow rapid preclinical benchmarking of existing vaccines against preclinical
350 vaccines with updated antigen designs.

351

322 **References**

- 323 1. Chand, M. *et al.* Investigation of novel SARS-COV-2 variant Variant of Concern 202012/01.
- 324 2. Davies, N. G. *et al.* Estimated transmissibility and impact of SARS-CoV-2 lineage B.1.1.7 in
- 325 England. *Science* eabg3055 (2021) doi:10.1126/science.abg3055.
- 326 3. Tegally, H. *et al.* *Emergence and rapid spread of a new severe acute respiratory syndrome-*
- 327 *related coronavirus 2 (SARS-CoV-2) lineage with multiple spike mutations in South Africa.*
- 328 <http://medrxiv.org/lookup/doi/10.1101/2020.12.21.20248640> (2020)
- 329 doi:10.1101/2020.12.21.20248640.
- 330 4. van Doremalen, N. *et al.* *Intranasal ChAdOx1 nCoV-19/AZD1222 vaccination reduces*
- 331 *shedding of SARS-CoV-2 D614G in rhesus macaques.*
- 332 <http://biorxiv.org/lookup/doi/10.1101/2021.01.09.426058> (2021)
- 333 doi:10.1101/2021.01.09.426058.
- 334 5. Port, J. R. *et al.* *SARS-CoV-2 disease severity and transmission efficiency is increased for*
- 335 *airborne but not fomite exposure in Syrian hamsters.*
- 336 <http://biorxiv.org/lookup/doi/10.1101/2020.12.28.424565> (2020)
- 337 doi:10.1101/2020.12.28.424565.
- 338 6. Muñoz-Fontela, C. *et al.* Animal models for COVID-19. *Nature* **586**, 509–515 (2020).
- 339 7. Tostanoski, L. H. *et al.* Ad26 vaccine protects against SARS-CoV-2 severe clinical disease
- 340 in hamsters. *Nat Med* **26**, 1694–1700 (2020).
- 341 8. Meyer, M. *et al.* *mRNA-1273 efficacy in a severe COVID-19 model: attenuated activation of*
- 342 *pulmonary immune cells after challenge.*
- 343 <http://biorxiv.org/lookup/doi/10.1101/2021.01.25.428136> (2021)
- 344 doi:10.1101/2021.01.25.428136.

- 345 9. Liu, Y. *et al.* Neutralizing Activity of BNT162b2-Elicited Serum — Preliminary Report. *N*
346 *Engl J Med* NEJMc2102017 (2021) doi:10.1056/NEJMc2102017.
- 347 10. Zhou, D. *et al.* Evidence of escape of SARS-CoV-2 variant B.1.351 from natural and vaccine
348 induced sera. *Cell* S0092867421002269 (2021) doi:10.1016/j.cell.2021.02.037.
- 349 11. Planas, D. *et al.* Sensitivity of infectious SARS-CoV-2 B.1.1.7 and B.1.351 variants to
350 neutralizing antibodies. <http://biorxiv.org/lookup/doi/10.1101/2021.02.12.430472> (2021)
351 doi:10.1101/2021.02.12.430472.
- 352 12. Wang, P. *et al.* Antibody Resistance of SARS-CoV-2 Variants B.1.351 and B.1.1.7.
353 <http://biorxiv.org/lookup/doi/10.1101/2021.01.25.428137> (2021)
354 doi:10.1101/2021.01.25.428137.
- 355 13. Wu, K. *et al.* mRNA-1273 vaccine induces neutralizing antibodies against spike mutants
356 from global SARS-CoV-2 variants. <http://biorxiv.org/lookup/doi/10.1101/2021.01.25.427948>
357 (2021) doi:10.1101/2021.01.25.427948.
- 358 14. Xie, X. *et al.* Neutralization of SARS-CoV-2 spike 69/70 deletion, E484K and N501Y
359 variants by BNT162b2 vaccine-elicited sera. *Nat Med* (2021) doi:10.1038/s41591-021-
360 01270-4.
- 361 15. Emary, K. R. W. *et al.* Efficacy of ChAdOx1 nCoV-19/AZD1222 Vaccine Against SARS-
362 CoV-2 VOC (B.1.1.7). *SSRN Journal* (2021) doi:10.2139/ssrn.3779160.
- 363 16. Hyams, C. *et al.* Assessing the Effectiveness of BNT162b2 and ChAdOx1nCoV-19 COVID-
364 19 Vaccination in Prevention of Hospitalisations in Elderly and Frail Adults: A Single
365 Centre Test Negative Case-Control Study. *Lancet*.

- 366 17. Cele, S. *et al.* *Escape of SARS-CoV-2 501Y.V2 from neutralization by convalescent plasma.*
367 <http://medrxiv.org/lookup/doi/10.1101/2021.01.26.21250224> (2021)
368 doi:10.1101/2021.01.26.21250224.
- 369 18. Greaney, A. J. *et al.* *Comprehensive mapping of mutations to the SARS-CoV-2 receptor-*
370 *binding domain that affect recognition by polyclonal human serum antibodies.*
371 <http://biorxiv.org/lookup/doi/10.1101/2020.12.31.425021> (2021)
372 doi:10.1101/2020.12.31.425021.
- 373 19. Madhi, S. A. *et al.* *Safety and efficacy of the ChAdOx1 nCoV-19 (AZD1222) Covid-19*
374 *vaccine against the B.1.351 variant in South Africa.*
375 <http://medrxiv.org/lookup/doi/10.1101/2021.02.10.21251247> (2021)
376 doi:10.1101/2021.02.10.21251247.
- 377 20. Janssen. Emergency Use Authorization (EUA) for an Unapproved Product Review
378 Memorandum.
- 379 21. McMahan, K. *et al.* Correlates of protection against SARS-CoV-2 in rhesus macaques.
380 *Nature* (2020) doi:10.1038/s41586-020-03041-6.
- 381 22. the Oxford COVID Vaccine Trial Group *et al.* T cell and antibody responses induced by a
382 single dose of ChAdOx1 nCoV-19 (AZD1222) vaccine in a phase 1/2 clinical trial. *Nat Med*
383 **27**, 270–278 (2021).
- 384 23. Sahin, U. *et al.* COVID-19 vaccine BNT162b1 elicits human antibody and TH1 T cell
385 responses. *Nature* **586**, 594–599 (2020).
- 386 24. Tarke, A. *et al.* Negligible impact of SARS-CoV-2 variants on CD4⁺ and CD8⁺ T cell
387 reactivity in COVID-19 exposed donors and vaccinees.

- 388 <http://biorxiv.org/lookup/doi/10.1101/2021.02.27.433180> (2021)
- 389 doi:10.1101/2021.02.27.433180.
- 390 25. Bricker, T. L. *et al.* *A single intranasal or intramuscular immunization with chimpanzee*
- 391 *adenovirus vectored SARS-CoV-2 vaccine protects against pneumonia in hamsters.*
- 392 <http://biorxiv.org/lookup/doi/10.1101/2020.12.02.408823> (2020)
- 393 doi:10.1101/2020.12.02.408823.
- 394 26. van Doremalen, N. *et al.* ChAdOx1 nCoV-19 vaccine prevents SARS-CoV-2 pneumonia in
- 395 rhesus macaques. *Nature* **586**, 578–582 (2020).
- 396 27. Rothe, C. *et al.* Transmission of 2019-nCoV Infection from an Asymptomatic Contact in
- 397 Germany. *The New England journal of medicine* (2020) doi:10/ggivr8.
- 398 28. Martin, M. Cutadapt removes adapter sequences from high-throughput sequencing reads.
- 399 *EMBnet j.* **17**, 10 (2011).
- 400 29. Langmead, B. & Salzberg, S. L. Fast gapped-read alignment with Bowtie 2. *Nat Methods* **9**,
- 401 357–359 (2012).
- 402 30. McKenna, A. *et al.* The Genome Analysis Toolkit: A MapReduce framework for analyzing
- 403 next-generation DNA sequencing data. *Genome Research* **20**, 1297–1303 (2010).
- 404 31. Avanzato, V. A. *et al.* Case Study: Prolonged Infectious SARS-CoV-2 Shedding from an
- 405 Asymptomatic Immunocompromised Individual with Cancer. *Cell* S0092867420314562
- 406 (2020) doi:10.1016/j.cell.2020.10.049.
- 407 32. Stadlbauer, D. *et al.* SARS-CoV-2 Seroconversion in Humans: A Detailed Protocol for a
- 408 Serological Assay, Antigen Production, and Test Setup. *Current Protocols in Microbiology*
- 409 **57**, (2020).

410 33. Wrapp, D. *et al.* Cryo-EM structure of the 2019-nCoV spike in the prefusion conformation.
411 *Science* **367**, 1260–1263 (2020).

412 34. Amanat, F. *et al.* A serological assay to detect SARS-CoV-2 seroconversion in humans. *Nat*
413 *Med* **26**, 1033–1036 (2020).

414

415 **Acknowledgments**

416 We would like to thank Mukul Ranjan, Sujatha Rashid, Kimberly Stemple, Alan Sutherland,
417 Anita Mora, Kizzmekia Corbett, Barney Graham, Florian Krammer, Fatima Amanat, Victoria
418 Avanzato, and the animal care takers for their assistance during the study. The following reagent
419 was obtained through BEI Resources, NIAID, NIH: SARS-Related Coronavirus 2, Isolate hCoV-
420 19/South Africa/KRISP-K005325/2020, NR-54009, contributed by Alex Sigal and Tulio de
421 Oliveira, and SARS-Related Coronavirus 2, Isolate hCoV-19/England/204820464/2020, NR-
422 54000, contributed by Bassam Hallis. Isolate hCoV-19/USA/MD-HP01542/2021 was obtained
423 from Andrew Pekosz, John Hopkins Bloomberg School of Public Health.

424 **Funding:** This work was supported by the Intramural Research Program of the National Institute
425 of Allergy and Infectious Diseases (NIAID), National Institutes of Health (NIH)
426 (1ZIAAI001179-01) and the Department of Health and Social Care using UK Aid funding
427 managed by the NIHR.

428 **Author contributions:** N.v.D. and V.J.M. designed the studies, S.C.G. and T.L. designed and
429 provided the vaccine, R.J.F., N.v.D., D.R.A., C.K.Y, J.R.P., M.G.H., J.E.S., B.N.W., T.T., K.B.,
430 S.L.A., S.R, B.J.S., D.L., C.M., G.S, E.d.W., and V.J.M. performed the experiments, R.J.F.,
431 N.v.D., D.R.A., C.K.Y, J.R.P., M.G.H., J.E.S., S.L.A., C.M., G.S, and V.J.M. analyzed results,
432 R.J.F., N.v.D and D.R.A. wrote the manuscript, all co-authors reviewed the manuscript.;

433 **Competing interests:** S.C.G. is a board member of Vaccitech and named as an inventor on a
434 patent covering the use of ChAdOx1-vector-based vaccines and a patent application covering a
435 SARS-CoV-2 (nCoV-19) vaccine (UK patent application no. 2003670.3). T.L. is named as an
436 inventor on a patent application covering a SARS-CoV-2 (nCoV-19) vaccine (UK patent
437 application no. 2003670.3). The University of Oxford and Vaccitech, having joint rights in the
438 vaccine, entered into a partnership with AstraZeneca in April 2020 for further development,
439 large-scale manufacture and global supply of the vaccine. Equitable access to the vaccine is a
440 key component of the partnership. Neither Oxford University nor Vaccitech will receive any
441 royalties during the pandemic period or from any sales of the vaccine in developing countries.
442 All other authors declare no competing interests.

443 **Materials and Correspondence:** All material requests should be sent to Vincent J. Munster,
444 vincent.munster@nih.gov.

445

446 **Materials and Methods**

447 *Ethics Statement*

448 All animal experiments were conducted in an AAALAC International-accredited facility and
449 were approved by the Rocky Mountain Laboratories Institutional Care and Use Committee
450 following the guidelines put forth in the Guide for the Care and Use of Laboratory Animals 8th
451 edition, the Animal Welfare Act, United States Department of Agriculture and the United States
452 Public Health Service Policy on the Humane Care and Use of Laboratory Animals.

453 The Institutional Biosafety Committee (IBC) approved work with infectious SARS-CoV-2 virus
454 strains under BSL3 conditions. Virus inactivation of all samples was performed according to

455 IBC-approved standard operating procedures for the removal of specimens from high
456 containment areas.

457 *Cells and virus*

458 SARS-CoV-2 variant B.1.351-1 (hCoV-19/South African/KRISP-K005325/2020,
459 EPI_ISL_678615) was obtained from Dr. Tulio de Oliveira and Dr. Alex Sigal at the Nelson R
460 Mandela School of Medicine, UKZN. SARS-CoV-2 variant B.1.1.7 (hCoV-
461 19/England/204820464/2020, EPI_ISL_683466) was obtained from Public Health England via
462 BEI. SARS-CoV-2 variant B.1.351-2 (USA/MD-HP01542/2021, EPI_ISL_890360) was
463 obtained from Andrew Pekosz at John Hopkins Bloomberg School of Public Health. Virus
464 propagation was performed in VeroE6 cells in DMEM supplemented with 2% fetal bovine
465 serum, 1 mM L-glutamine, 50 U/ml penicillin and 50 µg/ml streptomycin (DMEM2). VeroE6
466 cells were maintained in DMEM supplemented with 10% fetal bovine serum, 1 mM L-
467 glutamine, 50 U/ml penicillin and 50 µg/ml streptomycin. Mycoplasma testing is performed at
468 regular intervals and no mycoplasma was detected.

469 *Animal Experiments*

470 ChAdOx1 nCoV-19 was formulated as previously described²⁶. Four groups of 10, 4-6-week-old
471 female Syrian hamsters (Envigo Indianapolis, IN) were vaccinated with 2.5×10^8 infectious units
472 of ChAdOx1 nCoV-19 vaccine or ChAdOx1-GFP delivered intramuscularly in two 50 µL doses
473 into the posterior thighs 30 days prior to challenge. Five days prior to challenge a blood sample
474 was collected via the retro-orbital plexus under isoflurane anesthesia and spun at 2000 g for 10
475 min to obtain serum. Two groups (10 ChAdOx1 nCoV-19 vaccinated and 10 ChAdOx1 GFP
476 vaccinated hamsters) were challenged with 10^4 TCID₅₀/mL B.1.1.7 diluted in sterile Dulbecco's
477 Modified Eagle's media (DMEM), in a 40 µL bolus delivered intranasally, one-half into each

478 nostril. Two other groups (10 ChAdOx1 nCoV-19 vaccinated and 10 ChAdOx1 GFP vaccinated
479 hamsters) were similarly challenged with B.1.351-1 also diluted in sterile DMEM. Weights were
480 recorded daily until 14 DPI. Oropharyngeal swabs were collected daily in 1 mL of DMEM2 up
481 until 5 DPI. On 5 DPI 4 animals from each group were euthanized. The lungs were excised,
482 weighed, and photographed, and samples taken for qRT-PCR analysis, virus titrations and
483 histopathology. The remaining six animals in each group were monitored daily for signs of
484 disease and weighed until 14 DPI.

485 Two groups of 12 female Syrian hamsters (Envigo Indianapolis, IN) were vaccinated with $2.5 \times$
486 10^8 infectious units of ChAdOx1 nCoV-19 vaccine or ChAdOx1-GFP delivered intramuscularly
487 (IM group) in two 50 μ L doses into the posterior thighs or delivered intranasally (IN group) in 1
488 40 μ L dose delivered equally split between each nostril 60 days prior to challenge. One group of
489 10 naïve female hamsters was used as a control. All three groups were challenged with 10^4
490 TCID₅₀/mL B.1.351-2 diluted in sterile Dulbecco's Modified Eagle's media (DMEM), in a 40
491 μ L bolus delivered intranasally, equally split between each nostril. Weights were recorded daily
492 until 14 DPI. Oropharyngeal swabs were collected daily in 1 mL of DMEM2 up until 5 DPI. On
493 5 DPI 4 animals from each group were euthanized. The lungs were excised, weighed, and
494 samples taken for qRT-PCR analysis, virus titrations and histopathology. The remaining animals
495 in each group were monitored daily for signs of disease and weighed until 14 DPI.

496 *Virus titration*

497 Lung sections were weighed and homogenized in 1 mL of DMEM. Virus titrations were
498 performed by end-point titration of 10-fold dilutions of virus swab media or tissue homogenates
499 on VeroE6 cells in 96-well plates. When titrating tissue homogenate, the top 2 rows of cells were

500 washed 2 times with PBS prior to the addition of a final 100 μ l of DMEM2. Cells were incubated
501 at 37°C and 5% CO₂. Cytopathic effect was read 6 days later.

502 *Virus neutralization*

503 Sera were heat-inactivated (30 min, 56 °C). After an initial 1:10 dilution of the sera, two-fold
504 serial dilutions were prepared in DMEM2. 100 TCID₅₀ of SARS-CoV-2 variant B.1.1.7 or
505 B.1.351 was added to the diluted sera. After a 1hr incubation at 37°C and 5% CO₂, the virus-
506 serum mixture was added to VeroE6 cells. The cells were incubated for 6 days at 37°C and 5%
507 CO₂ at which time they were evaluated for CPE. The virus neutralization titer was expressed as
508 the reciprocal value of the highest dilution of the serum that still inhibited virus replication.

509 *RNA extraction and quantitative reverse-transcription polymerase chain reaction*

510 RNA was extracted from oropharyngeal swabs using the QiaAmp Viral RNA kit (Qiagen)
511 according to the manufacturer's instructions and following high containment laboratory
512 protocols. Lung samples were homogenized and extracted using the RNeasy kit (Qiagen)
513 according to the manufacturer's instructions and following high containment laboratory
514 protocols. A viral sgRNA²⁷ specific assay was used for the detection of viral RNA. Five μ L of
515 extracted RNA was tested with the Quantstudio 3 system (Thermofisher) according to
516 instructions from the manufacturer. A standard curve was generated during each run using
517 SARS-CoV-2 standards containing a known number of genome copies.

518 *Viral RNA sequencing*

519 For sequencing from viral stocks, sequencing libraries were prepared using Stranded Total RNA
520 Prep Ligation with Ribo-Zero Plus kit per manufacturer's protocol (Illumina) and sequenced on
521 an Illumina MiSeq at 2 x 150 base pair reads. For sequencing from swab and lung tissue, total
522 RNA was depleted of ribosomal RNA using the Ribo-Zero Gold rRNA Removal kit (Illumina).

523 Sequencing libraries were constructed using the KAPA RNA HyperPrep kit following
524 manufacturer's protocol (Roche Sequencing Solutions). To enrich for SARS-CoV-2 sequence,
525 libraries were hybridized to myBaits Expert Virus biotinylated oligonucleotide baits following
526 the manufacturer's manual, version 4.01 (Arbor Biosciences, Ann Arbor, MI). Enriched libraries
527 were sequenced on the Illumina MiSeq instrument as paired-end 2 X 151 base pair reads. Raw
528 fastq reads were trimmed of Illumina adapter sequences using cutadapt version 1.12²⁸ and then
529 trimmed and filtered for quality using the FASTX-Toolkit (Hannon Lab, CSHL). Remaining
530 reads were mapped to the SARS-CoV-2 2019-nCoV/USA-WA1/2020 genome (MN985325.1) or
531 hCoV-19/England/204820464/2020 (EPI_ISL_683466) or hCoV-19/SouthAfrica/KRISP-
532 K005325/2020 (EPI_ISL_678615) using Bowtie2 version 2.2.9²⁹ with parameters --local --no-
533 mixed -X 1500. PCR duplicates were removed using picard MarkDuplicates (Broad Institute)
534 and variants were called using GATK HaplotypeCaller version 4.1.2.0³⁰ with parameter -ploidy
535 2. Variants were filtered for QUAL > 500 and DP > 20 using bcftools.

536 *Expression and purification of SARS-CoV-2 S and receptor binding domain*

537 Protein production was performed as described previously^{31,32}. Expression plasmids encoding the
538 codon optimized SARS-CoV-2 full length S and RBD were obtained from Kizzmekia Corbett
539 and Barney Graham (Vaccine Research Center, Bethesda, USA)³³ and Florian Krammer (Icahn
540 School of Medicine at Mt. Sinai, New York, USA)³⁴. Expression was performed in Freestyle
541 293-F cells (Thermofisher), maintained in Freestyle 293 Expression Medium (Gibco) at 37°C
542 and 8% CO₂ shaking at 130 rpm. Cultures totaling 500 mL were transfected with PEI at a
543 density of one million cells per mL. Supernatant was harvested 7 days post transfection, clarified
544 by centrifugation and filtered through a 0.22 µm membrane. The protein was purified using Ni-
545 NTA immobilized metal-affinity chromatography (IMAC) using Ni Sepharose 6 Fast Flow Resin

546 (GE Lifesciences) or NiNTA Agarose (QIAGEN) and gravity flow. After elution the protein was
547 buffer exchanged into 10 mM Tris pH8, 150 mM NaCl buffer (S) or PBS (RBD) and stored at –
548 80°C.

549 *ELISA*

550 ELISA was performed as described previously²⁶. Briefly, maxisorp plates (Nunc) were coated
551 overnight at 4°C with 50 ng/well S or RBD protein in PBS. Plates were blocked with 100 µl of
552 casein in PBS (Thermo Fisher) for 1hr at RT. Serum diluted 1:6,400 was further 2-fold serially
553 diluted in casein in PBS was incubated at RT for 1hr. Antibodies were detected using affinity-
554 purified polyclonal antibody peroxidase-labeled goat-anti-monkey IgG (Seracare, 074-11-021) in
555 casein followed by TMB 2-component peroxidase substrate (Seracare, 5120-0047). The reaction
556 was stopped using stop solution (Seracare, 5150-0021) and read at 450 nm. All wells were
557 washed 4x with PBST 0.1% tween in between steps. Threshold for positivity was set at 2x OD
558 value of negative control (serum obtained from unvaccinated hamsters prior to start of the
559 experiment).

560 *Data availability statement*

561 Data have been deposited in Figshare 10.6084/m9.figshare.14210879.

562

563 **References Materials and Methods**

564 25. van Doremalen, N. *et al.* ChAdOx1 nCoV-19 vaccine prevents SARS-CoV-2 pneumonia in
565 rhesus macaques. *Nature* **586**, 578–582 (2020).

566 26. Corman, V. M. *et al.* Detection of 2019 novel coronavirus (2019-nCoV) by real-time RT-
567 PCR. *Eurosurveillance* **25**, (2020).

- 568 27. Rothe, C. *et al.* Transmission of 2019-nCoV Infection from an Asymptomatic Contact in
569 Germany. *The New England journal of medicine* (2020) doi:10/ggjvr8.
- 570 28. Avanzato, V. A. *et al.* Case Study: Prolonged Infectious SARS-CoV-2 Shedding from an
571 Asymptomatic Immunocompromised Individual with Cancer. *Cell* S0092867420314562
572 (2020) doi:10.1016/j.cell.2020.10.049.
- 573 29. Stadlbauer, D. *et al.* SARS-CoV-2 Seroconversion in Humans: A Detailed Protocol for a
574 Serological Assay, Antigen Production, and Test Setup. *Current Protocols in Microbiology*
575 **57**, (2020).
- 576 30. Wrapp, D. *et al.* Cryo-EM structure of the 2019-nCoV spike in the prefusion conformation.
577 *Science* **367**, 1260–1263 (2020).
- 578 31. Amanat, F. *et al.* A serological assay to detect SARS-CoV-2 seroconversion in humans. *Nat*
579 *Med* **26**, 1033–1036 (2020).